Received: 26 May 2023 | Accepted: 4 August 2023

DOI: 10.1111/2041-210X.14204

Methods in Ecology and Evolution

RESEARCH ARTICLE

Mind the uncertainty: Global plate model choice impacts deep-time palaeobiological studies

Lucas Buffan[1,2] | Lewis A. Jones[1] | Mathew Domeier[3,4] | Christopher R. Scotese[5] | Sabin Zahirovic[6] | Sara Varela[1]

[1]Centro de Investigación Mariña, Grupo de Ecoloxía Animal, Universidade de Vigo, Vigo, Spain; [2]Département de Biologie, École Normale Supérieure de Lyon, Université Claude Bernard Lyon 1, Lyon Cedex 07, France; [3]Centre for Earth Evolution and Dynamics (CEED), University of Oslo, Oslo, Norway; [4]Centre for Planetary Habitability (PHAB), University of Oslo, Oslo, Norway; [5]Department of Earth and Planetary Sciences, Northwestern University, Evanston, Illinois, USA and [6]EarthByte Group, School of Geosciences, University of Sydney, Sydney, New South Wales, Australia

Correspondence
Lucas Buffan
Email: lucas.l.buffan@gmail.com

Lewis A. Jones
Email: lewisalan.jones@uvigo.es

Funding information
AuScope National Collaborative Research Infrastructure System (NCRIS) program; Australian Research Council, Grant/Award Number: DE210100084; École Normale Supérieure de Lyon; H2020 European Research Council, Grant/Award Number: 947921; Juan de la Cierva-formación 2021 fellowship, Grant/Award Number: FJC2021-046695-I; Universidade de Vigo; CISUG

Handling Editor: Gustavo Burin

Abstract

1. Global plate models (GPMs) aim to reconstruct the tectonic evolution of the Earth by modelling the motion of the plates and continents through time. These models enable palaeobiologists to study the past distribution of extinct organisms. However, different GPMs exist that vary in their partitioning of the Earth's surface and the modelling of continental motions. Consequently, the preferred use of one GPM will influence palaeogeographic reconstruction of fossil occurrences and any inferred palaeobiological and palaeoclimatic conclusion.
2. Here, using five open-access GPMs, we reconstruct the palaeogeographic distribution of cell centroids from a global hexagonal grid and quantify palaeogeographic uncertainty across the entire Phanerozoic (540–0 Ma). We measure uncertainty between reconstructed coordinates using two metrics: (1) palaeolatitudinal standard deviation and (2) mean pairwise geodesic distance. Subsequently, we evaluate the impact of GPM choice on palaeoclimatic reconstructions when using fossil occurrence data. To do so, we use two climatically sensitive entities (coral reefs and crocodylomorphs) to infer the palaeolatitudinal extent of subtropical climatic conditions for the last 240 million years.
3. Our results indicate that differences between GPMs increase with the age of reconstruction. Specifically, cell centroids rotated to older intervals show larger differences in palaeolatitude and geographic spread than those rotated to younger intervals. However, high palaeogeographic uncertainty is also observed in younger intervals within tectonically complex regions (i.e. in the vicinity of terrane and plate boundaries). We also show that when using fossil data to infer the distribution of subtropical climatic conditions across the last 240 Ma, estimates vary by 6–7° latitude on average, and up to 24° latitude in extreme cases.

Lucas Buffan and Lewis A. Jones are contributed equally to this work

4. Our findings confirm that GPM choice is an important consideration when studying past biogeographic patterns and palaeoclimatic trends. We recommend using GPMs that report true palaeolatitudes (i.e. use a palaeomagnetic reference frame) and incorporating palaeogeographic uncertainty into palaeobiological analyses.

KEYWORDS
coral reefs, crocodiles, global plate models, macroecology, palaeobiogeography, palaeobiology, palaeoclimate, palaeogeography, Phanerozoic

1 | INTRODUCTION

Akin to neontologists, palaeobiologists seek to understand the origin, distribution and extinction of species across time and space (e.g. Alroy, 2014; Boddy et al., 2022; Meseguer & Condamine, 2020; Powell et al., 2015; Spano et al., 2016). However, while neontologists can study the present-day geographic distribution of taxa, palaeobiologists must contend with the shift of the continents over geological timescales. Specifically, the geographic location of fossil occurrences on the Earth's surface today does not necessarily represent their location in vivo; fossil remains found at tropical latitudes might have been deposited at temperate latitudes and vice versa. Consequently, reconstructing the past geographic distribution—that is, the palaeogeographic distribution—of fossil occurrences is fundamental to the study of macroecological patterns in deep time. To do so, palaeobiologists routinely use what are known as global plate models (e.g. Allen et al., 2020; Antell et al., 2020; Boddy et al., 2022; Brocklehurst et al., 2017; Dunne et al., 2020; Jones et al., 2022; Zhang et al., 2022).

Global plate models (GPMs) aim to reconstruct the tectonic evolution of the Earth, modelling the motion of the continents across its surface through geological time. They do so using Euler's rotation theorem to describe the motion of geometries—such as tectonic plates or geological terranes—on a sphere (McKenzie & Parker, 1967; Morgan, 1968). Since the 1970s, numerous GPMs have been developed by both the scientific community (e.g. Domeier & Torsvik, 2014; Golonka, 2007; Golonka et al., 1994; Matthews et al., 2016; Merdith et al., 2021; Müller et al., 1993, 2019; Scotese et al., 1988; Scotese & Wright, 2018; Seton et al., 2012; Torsvik & Cocks, 2017; Torsvik, Van der Voo, et al., 2008; Vérard, 2019; Young et al., 2019) and industry (e.g. Getech plc and Robertson Research) for purposes such as geological resource exploration (Markwick, 2019) and Earth system modelling (Lunt et al., 2016). A more recent shift to 'full-plate models' (e.g. Merdith et al., 2021) and deforming plate models (e.g. Gurnis et al., 2018; Müller et al., 2019) has increased the complexity of GPMs by describing—in detail—how plate boundaries and deforming regions have evolved through time (Seton et al., 2023).

A GPM is made up of two key components. The first component is a set of 'geometries' dividing the surface of the Earth into individual tectonic elements that can be independently reconstructed. These elements include both 'dynamic polygons' (also known as 'continuously closing plate polygons'), which change shape through time, and 'static polygons', whose shape and size are fixed. The former are used to model entire tectonic plates, whereas the latter are used to delineate continents, fault-bound tectonic blocks ('terranes') or any other arbitrary parcel of crust whose shape and size can be treated as fixed through the modelled time. Whether any given continent or crustal block can be appropriately treated as a static polygon depends on the spatial resolution and timescale being considered, and so the number and definition of static polygons can vary significantly between GPMs (with more recent and temporally more extensive GPMs tending to have more static polygons), resulting in differential partitioning of the Earth's surface (Figure **S1**). Differences in the polygonisation of the Earth's surface between GPMs also arise from different interpretations about the locations of ancient tectonic boundaries—which occurs more frequently in complicated geological areas and in deeper time (see Vérard, 2019 for additional discussion).

The second key component of a GPM is a rotation file that describes the time-dependent motion of the tectonic elements as finite Euler rotations (Domeier & Torsvik, 2019; Müller et al., 2018). These rotation files can be read and interpolated by software programs such as *GPlates* (Müller et al., 2018) to reconstruct the motion of the tectonic elements through time, and enable the reconstruction of palaeocoordinates for fossil occurrence data (Boyden et al., 2011; Wright et al., 2013). It is important to note that rotation files can report the motion of tectonic elements with respect to one another ('relative' motion) and/or with respect to the Earth's mantle or the planetary spin-axis (so-called 'absolute' motion) (Torsvik, Van der Voo, et al., 2008). Only the latter reference frame (the motion of tectonic elements relative to Earth's spin-axis) is appropriate for the reconstruction of fossil occurrence data as it reports true palaeolatitudes (Seton et al., 2023). Without the use of such reference frames, palaeocoordinates are likely to be meaningless for the study of past geographic distributions. Recent work has demonstrated differences in the palaeogeographic reconstruction of several fossil and geological data sets when using different GPMs (e.g. Boddy et al., 2022; Cao et al., 2019; Jones et al., 2022). Yet, the impact of model choice on palaeogeographic reconstructions at global Phanerozoic scale remains untested.

Quantifying this 'palaeogeographic uncertainty' is key to understanding the robustness of observed deep-time biodiversity patterns and their response to past climatic change (e.g. Mannion et al., 2014; Reddin et al., 2018). Here, we quantify spatial

discrepancies in palaeogeographic reconstruction from five open-access GPMs. To do so, we reconstruct the palaeogeographic coordinates (i.e. palaeocoordinates) of centroids from a global hexagonal grid (~100 km spacing) across the last 540 million years (Myr). By comparing these five reconstructions, we identify key spatial zones and timeframes of palaeogeographic uncertainty. Subsequently, we reconstruct the palaeogeographic distribution of two climatically sensitive entities (fossil coral reefs and terrestrial crocodylomorphs) to evaluate the impact of GPM choice on estimations of the palaeolatitudinal extent of tropical climatic conditions over the last 240 Myr. We hypothesise that: (1) differences in palaeogeographic reconstruction increase with age, and (2) GPM choice can significantly influence reconstructions of palaeogeographic distributions of organisms and inferred palaeoclimatic conditions.

2 | MATERIALS AND METHODS

2.1 | Global plate models

Five open-access global plate models (GPMs) were used to evaluate spatiotemporal differences in palaeogeographic reconstructions: WR13 (Wright et al., 2013), MA16 (Matthews et al., 2016), TC17 (Torsvik & Cocks, 2017), SC16 (Scotese, 2016; Scotese & Wright, 2018) and ME21 (Merdith et al., 2021). These GPMs have variable temporal coverage (see Table 1) with WR13, SC16, TC17 and ME21 covering the entirety of our Phanerozoic study period (540–0 Ma), while MA16 is limited to the Devonian–Recent (410–0 Ma).

WR13 and SC16 both share a common lineage stemming from the plate model of Scotese (2004), but WR13 employed modifications to fit palaeomagnetic data summarised in Torsvik and Van der Voo (2002). The Scotese GPM has evolved slowly over the last three decades. Small, but significant, changes have occurred in the location of the core continents (e.g. North America, Europe, Gondwana), whereas major changes have occurred in the placement of North China, South China, Cimmeria and the exotic terranes of western North America (Figure S2). The time range of the Scotese GPM has also been extended further into the Precambrian (Scotese, 2004, 2016; Scotese & Elling, 2017). More recently, SC16 has also been used to produce a set of Phanerozoic palaeogeographic maps and digital elevation models (Scotese & Wright, 2018). TC16 primarily stems from the global palaeomagnetic model of Torsvik et al. (2012), but it incorporates some changes made in the subsequent plate models of Domeier and Torsvik (2014) for the late Palaeozoic (410–250 Ma), and Domeier (2016) in the earlier Palaeozoic (500–410 Ma). Note that TC16 is presented in a mantle reference frame by default, but here we use the version which is available in the palaeomagnetic reference frame. The model of MA16 is likewise built upon the model of Domeier and Torsvik (2014) for the late Palaeozoic (410–250), and so MA16 and TC16 are very similar for that interval of time. For Mesozoic and Cenozoic time, MA16 is based on the model of Müller et al. (2016). Note that the model of Müller et al. (2016) exists in a mantle reference frame, and so too does the original model of MA16 for times between 250 and 0 Ma. However, a version cast into the palaeomagnetic reference frame was subsequently made available, using the global apparent polar wander path from Torsvik et al. (2012), and here we utilise this later version. ME21 is largely a composition of several pre-existing models, namely the model of Merdith et al. (2017) from 1000 to 500 Ma, the models of Domeier (2016, 2018) for the early Palaeozoic (500–410 Ma) and a modified version of Young et al. (2019) for the interval 410–0 Ma, and the entire 1000–0 Ma model interval is cast into a palaeomagnetic reference frame. The model of Young et al. (2019) is modified from Matthews et al. (2016), which again was built from Domeier and Torsvik (2014) for the late Palaeozoic interval (410–250 Ma) and Müller et al. (2016) from 230 to 0 Ma. Thus, for the Palaeozoic interval (particularly the late Palaeozoic), there is some common ancestry between TC16, MA16 and ME21, and this extends into the Mesozoic and Cenozoic for MA16 and ME21. Nevertheless, the modifications made between these alternative models is a reflection of outstanding palaeogeographic uncertainty. Figure 1 summarises the main interrelationships between these various GPMs.

2.2 | Quantifying spatiotemporal differences

To quantify differences in palaeogeographic reconstruction (Figure 2), we first generated a discrete global hexagonal grid

TABLE 1 A summary table of the global plate models used in this study. The table includes the abbreviations used in this study, the names of models according to the GPlates Web Service (https://gwsdoc.gplates.org), the temporal coverage of each model and the relevant reference for each model. Note, all these models provide absolute motions in a palaeomagnetic reference frame, which is essential for reconstructing the palaeogeographic distribution of fossil occurrence data to ensure true palaeolatitudes.

Abbreviation	GPlates ID	Temporal coverage	Reference
WR13	GOLONKA	0–550 Ma	Wright et al. (2013)
MA16	MATTHEWS2016_pmag_ref	0–410 Ma	Matthews et al. (2016)
TC17	TorsvikCocks2017	0–540 Ma	Torsvik and Cocks (2017)
SC16	PALEOMAP	0–1100 Ma	Scotese (2016) and Scotese and Wright (2018)
ME21	MERDITH2021	0–1000 Ma	Merdith et al. (2021)

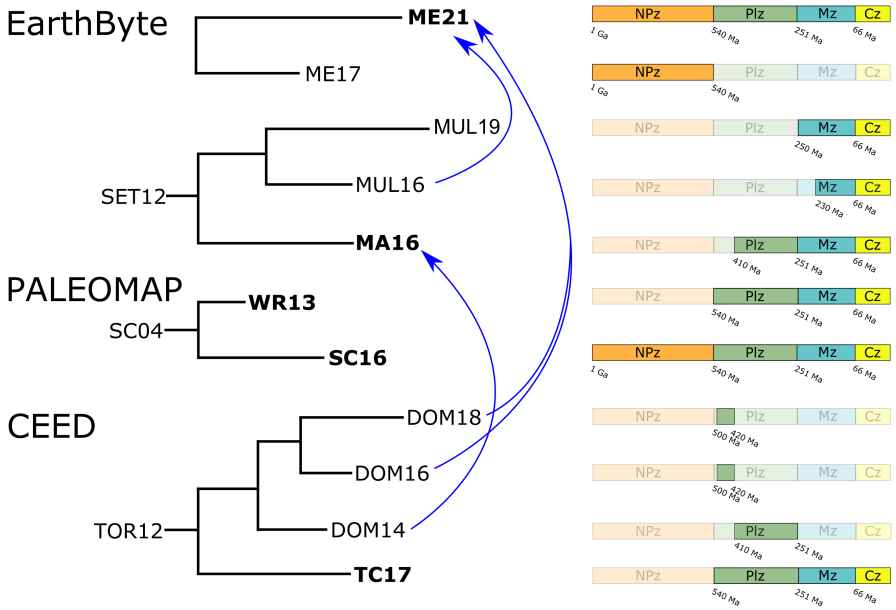

FIGURE 1 A 'cladogram'-type representation of the relationship between global plate models from three independent palaeogeographic model development groups (EarthByte, PALEOMAP project and Centre for Earth Evolution and Dynamics [CEED]) used in this study, and their respective temporal coverage. Blue arrows indicate 'horizontal transfers' between models, that is, amalgamations of models from different groups. Global plate model abbreviations: TOR12 (Torsvik et al., 2012), DOM14 (Domeier & Torsvik, 2014), TC17 (Torsvik & Cocks, 2017), DOM16 (Domeier, 2016), DOM18 (Domeier, 2018), MA16 (Matthews et al., 2016), ME17 (Merdith et al., 2017), ME21 (Merdith et al., 2021), MUL16 (Müller et al., 2016), MUL19 (Müller et al., 2019), SC04 (Scotese, 2004), SC16 (Scotese, 2016; Scotese & Wright, 2018), SET12 (Seton et al., 2012), WR13 (Wright et al., 2013). Models included in this study are represented in bold. Era abbreviations: Cenozoic (Cz), Mesozoic (Mz), Palaeozoic (Plz) and Neo-Proterozoic (NPz).

(~100 km spacings; World Geodetic System 1984) via the python library 'h3' v.3.7.6 (Uber, 2023). This hexagonal grid avoids sampling biases in the polar regions associated with the geographic coordinate system. Most GPMs have a network of static polygons covering most of the Earth's continental areas, and we retained only the present-day grid cells that were included within a static polygon in each of the GPMs. Subsequently, we reconstructed palaeocoordinates for cell centroids across the last 540 Myr with a time step of 10 Myr for each GPM, resulting in up to 54 time steps depending on GPM (Table 1). To do so, we used the python library 'pygplates' ver. 0.36.0 (Williams et al., 2017) to interact with the software GPlates (Boyden et al., 2011; Müller et al., 2018). Using the reconstructed palaeocoordinates for each cell—from each model—we calculated: (1) the standard deviation (SD) in palaeolatitude and (2) the mean pairwise geodesic distance (PGD) between reconstructed coordinates (up to five sets) for each cell. The former of these quantifies the potential uncertainty in palaeolatitude between models with significance for studies such as those focused on reconstructing the latitudinal biodiversity gradient in deep time (e.g. Allen et al., 2020; Song et al., 2020). The latter quantifies the uncertainty in palaeogeographic position between models having significance for studies focused on themes such as reconstructing organisms' geographic range sizes (e.g. Antell et al., 2020). Mean PGD was calculated using the R package 'geosphere' ver. 1.5-18 (Hijmans et al., 2021).

2.3 | Palaeoclimatic reconstruction

To test the influence of GPM choice on fossil-based palaeoclimatic reconstructions, we estimate the palaeolatitudinal extent of (sub-) tropical climatic conditions using two climatically sensitive entities: warm-water coral reefs and terrestrial crocodylomorphs (Figure S3). These entities are frequently used to infer the extent of (sub-)tropical palaeoclimatic conditions due to their limited thermal tolerance and geographic distribution today (e.g. Burgener et al., 2023; Markwick, 2007). Fossil crocodylomorph occurrences (="Crocodylomorpha") were downloaded from The Paleobiology Database (https://paleobiodb.org/#/) on 9 November 2022 and were restricted to terrestrial taxa and body fossils. Marine taxa were excluded as they appear to be less constrained by climatic factors than terrestrial taxa (Mannion et al., 2015). Fossil coral reef occurrences were downloaded from the PaleoReef Database (Kiessling & Krause, 2022) on 10 March 2022 and were restricted to scleractinian 'true reefs' with a tropical affinity. This led us to exclude pre-Anisian reef occurrences. At the end of the cleaning, the midpoint age of oldest crocodylomorph occurrence was 232.5 Ma, and the oldest reef occurrence was 231.5 Ma. Finally, fossil occurrences were split into 10 Myr time bins using the midpoint age of each occurrence's age range. After data processing, 4638 terrestrial crocodylomorphs and 419 warm-water coral reef occurrences remained for analyses.

Using the five GPMs (Table 1), we reconstructed the palaeocoordinates (i.e. palaeogeographic location) for each fossil occurrence using

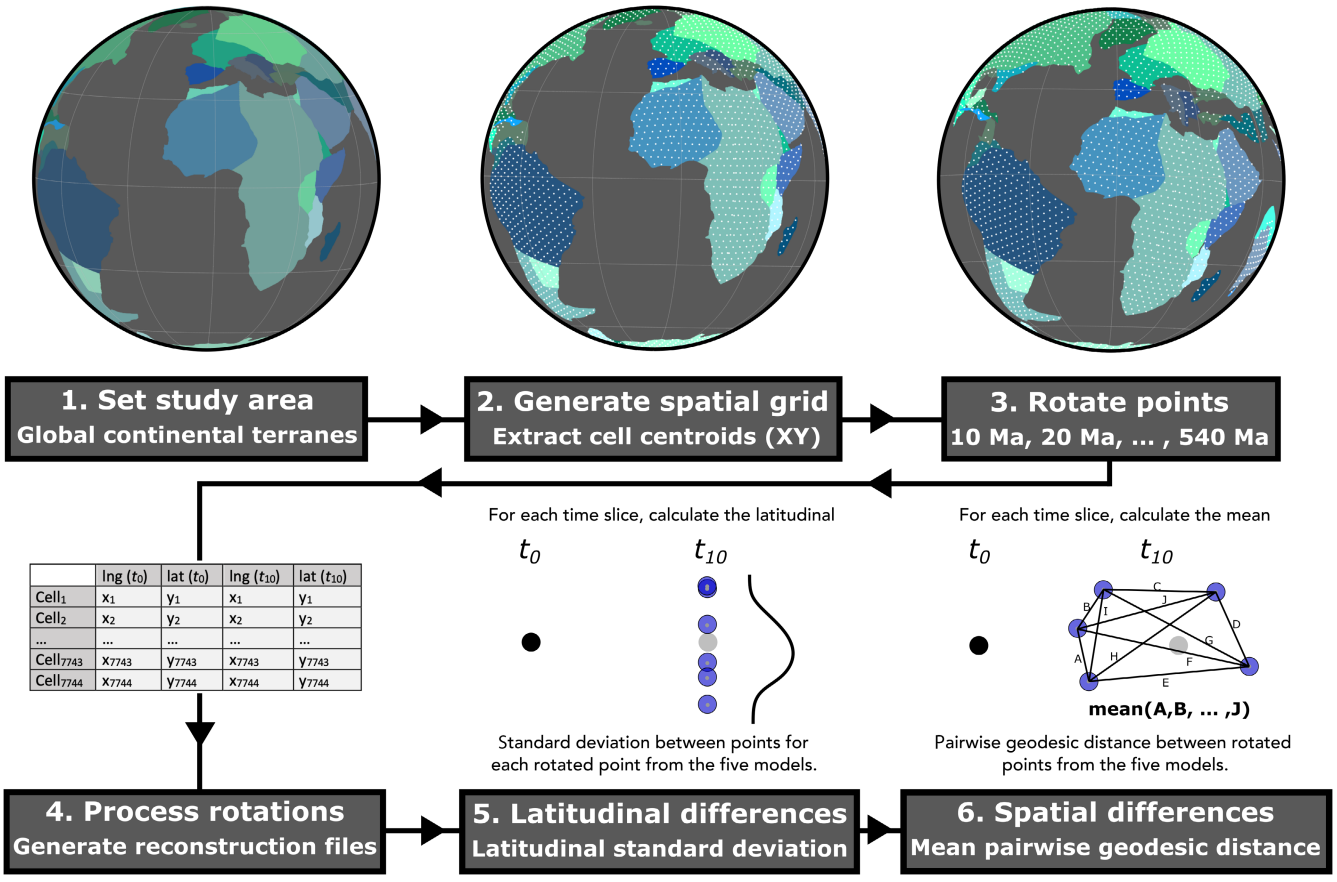

	lng (t_0)	lat (t_0)	lng (t_{10})	lat (t_{10})
$Cell_1$	x_1	y_1	x_1	y_1
$Cell_2$	x_2	y_2	x_2	y_2
...	...	...	...	...
$Cell_{7743}$	x_{7743}	y_{7743}	x_{7743}	y_{7743}
$Cell_{7744}$	x_{7744}	y_{7744}	x_{7744}	y_{7744}

FIGURE 2 A graphical schematic of the simulation workflow used in this study. Using continental tectonic elements, the study area is first established (1). Subsequently, a discrete global hexagonal grid (~100 km spacings) is generated via the python library 'h3' v.3.7.6 (Uber, 2023) and cell centroids extracted for cells intersecting with the continental tectonic elements (2). Cell centroids are then rotated (3) at time intervals of 10 Myr throughout the Phanerozoic (540–0 Ma), for each model, using the software GPlates via the 'pygplates' ver. 0.36.0 python library (Williams et al., 2017). Reconstruction files are subsequently generated for each model (4), and the palaeolatitudinal standard deviation (5) and the mean pairwise geodesic distance (6) calculated for each cell centroid between the five models for each time step. Note, the black and grey point in panels 5 and 6 depict the present-day location of a sample. The blue points indicate the palaeogeographic location of the sample for each Global Plate Model.

the midpoint age of the occurrence's respective age range as the reconstruction time. Assuming hemispheric symmetry in climatic conditions, we subsequently identified the maximum absolute palaeolatitude (i.e. most poleward occurrence) within each time bin—for each model and entity—to infer the palaeolatitudinal extent of (sub-)tropical climatic conditions. Using this deduction, we quantified the potential uncertainty in the palaeolatitudinal extent of (sub-)tropical climatic conditions by calculating the palaeolatitudinal range between estimates for each time bin, that is, between the most poleward occurrences for each model. Finally, for each fossil occurrence, we calculated the median, maximum and minimum reconstructed palaeolatitude from the five model estimates.

3 | RESULTS

3.1 | Spatiotemporal discrepancy trends

Palaeolatitudinal SD and mean PGD demonstrate an increasing uncertainty in palaeogeographic reconstruction with age (Figures 3 and 4; Figure S4). Overall, GPMs are in good agreement for the last 100 Myr (mid-Cretaceous–Recent), with 97.4% of cells having a palaeolatitudinal SD less than 5° and a mean PGD less than 1000 km (Figure 3). However, GPM reconstructions begin to substantially diverge at greater reconstruction ages with generally increasing uncertainty throughout the Mesozoic (251.9–66 Ma) and Palaeozoic (538.8–251.9 Ma). For example, in the Cenozoic (66–0 Ma), 1.9% of cells have a palaeolatitudinal SD of more than 5°, going up to 14.8% of cells during the Mesozoic and 53.8% during the Palaeozoic (Figure 3a). This trend is further reflected by an increase in mean PGD with 1.2% of cells having a value of more than 1000 km in the Cenozoic, 20.2% during the Mesozoic and 80% during the Palaeozoic (Figure 3b). Differences in Cambrian (538.8–485.4 Ma) reconstructions are especially large, with a considerable proportion of cells having a palaeolatitudinal SD of more than 5° (~76.3%) and mean PGD of more than 1000 km (~90.1%) (Figure 3; Figure S4). Notably, despite this overall trend of increasing palaeogeographic uncertainty with age, uncertainty is relatively low during the latest Carboniferous and Permian in comparison to the rest of the Palaeozoic and early Mesozoic (Figure 3).

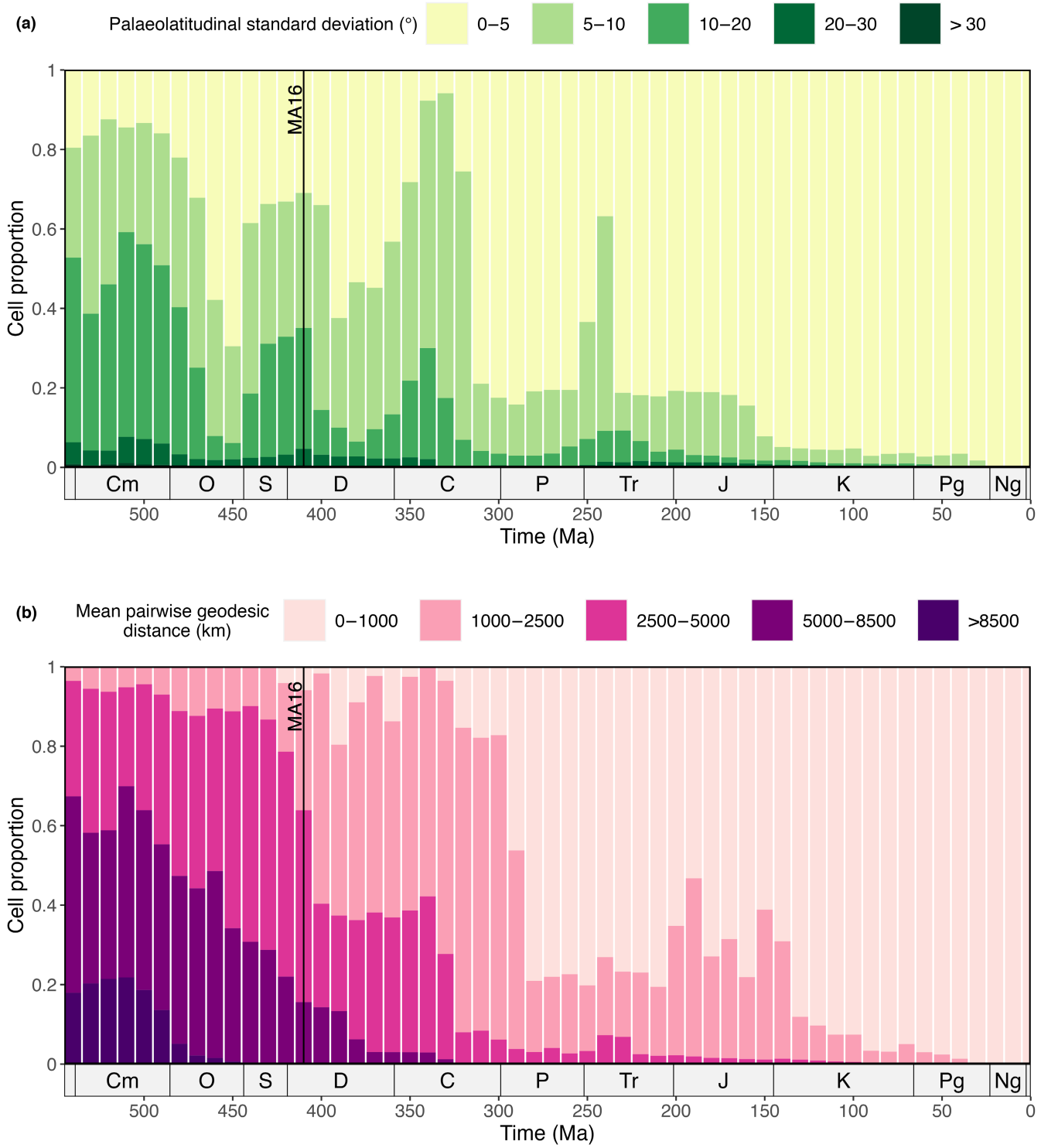

FIGURE 3 Phanerozoic trends in spatial discrepancies between Global Plate Models within 10 Myr time steps. Values are categorised and depicted as proportions of cells. (a) Palaeolatitudinal standard deviation between reconstructed palaeocoordinates for cell centroids. (b) Mean pairwise geodesic distance between reconstructed palaeocoordinates for cell centroids. The black line depicts the temporal limit (410 Ma) of the MA16 model (Matthews et al., 2016). The bar plots show increasing palaeogeographic uncertainty between models with age of reconstruction. Period abbreviations are as follows: Cambrian (Cm); Ordovician (O), Silurian (S), Devonian (D), Carboniferous (C), Permian (P), Triassic (Tr), Jurassic (J), Cretaceous (K), Paleogene (Pg) and Neogene (Ng). The Quaternary is not depicted. The geological time scale axis was added to the plot using the R package 'deeptime' ver. 1.0.1 (Gearty, 2023).

Our palaeolatitudinal SD and mean PGD results show palaeogeographic uncertainty is not evenly distributed in space (Figure 4; Figure S4). High palaeogeographic uncertainty is generally restricted to plate boundaries and active deformation zones during the Cenozoic and Mesozoic but extends to broader areas during the Palaeozoic (Figure 4; Figure S4; supplementary GIFs Buffan et al., 2023).

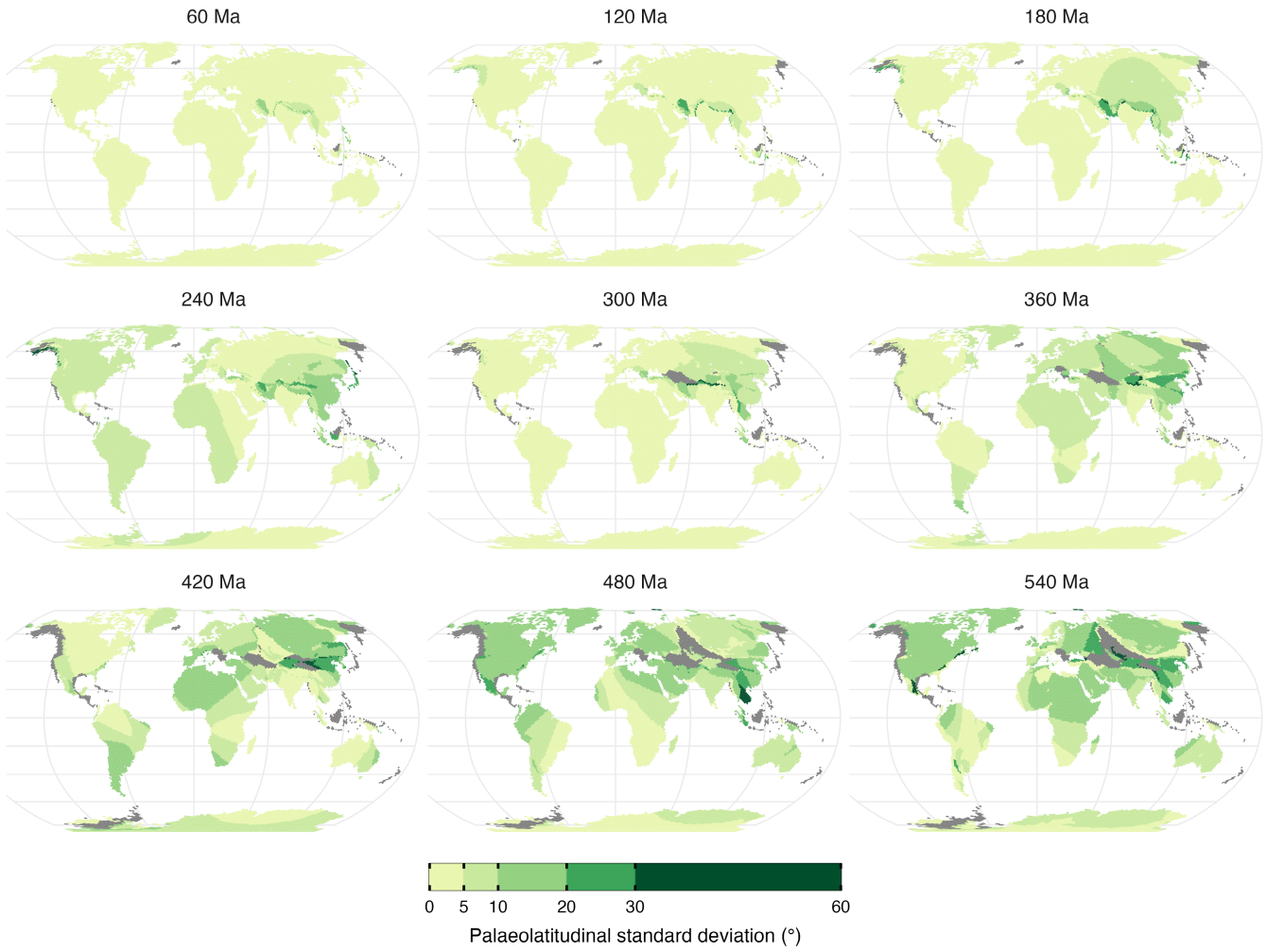

FIGURE 4 Categorised maps of the palaeolatitudinal standard deviation between reconstructed palaeocoordinates of cell centroids from global plate models. Values are mapped onto a present-day map with darker shades indicating greater palaeolatitudinal standard deviation between palaeocoordinates. Grey cells denote areas where palaeocoordinates could not be reconstructed at time of reconstruction for cell centroids by at least two models. Maps are presented in the Robinson projection (ESRI:54030).

For example, throughout the Cenozoic and Mesozoic, palaeogeographic reconstructions of South American cell centroids appear well constrained in comparison to those along the Eurasian–Indian and Eurasian–Arabian plate boundaries (Figure 4; Figure S4; supplementary GIFs Buffan et al., 2023).

3.2 | Palaeoclimatic reconstructions

Our results suggest that reconstructions of the palaeolatitudinal extent of (sub-)tropical climatic conditions—based on terrestrial crocodylomorphs and coral reef occurrences—can vary by up to 12.3° latitude in crocodylomorphs and 24.1° in coral reefs, depending on GPM choice (Figure 5). The average range between models along the 240 Myr time series is 7.7° for coral reefs and 6.5° for terrestrial crocodylomorphs (Figure 5). However, despite these large observed differences, the direction of change (equatorward vs. poleward) in the extent of (sub-)tropical conditions is largely consistent between GPMs (Figure 5). Both time series exhibit a significant positive correlation between age of reconstruction and the range in the extent of (sub-)tropical conditions from GPM estimates (Pearson's correlation test: $R=0.43$; $p=0.05$ for coral reefs and $R=0.55$; $p=0.005$ for crocodylomorphs). Comparisons of reconstructed palaeocoordinates for all occurrences further support an increase in palaeolatitudinal uncertainty with age (Figure S6). For example, the average palaeolatitudinal range between the five GPMs for each occurrence—within each time bin—increases significantly with age (Pearson's correlation test: $R=0.49$; $p<0.001$ for coral reefs and $R=0.33$; $p<0.001$ for crocodylomorphs).

4 | DISCUSSION

4.1 | With age comes uncertainty

In this study, we quantified palaeogeographic reconstruction differences between five global plate models (GPMs). Our results demonstrate that palaeogeographic uncertainty increases with age (Figure 3) suggesting caution is required when reconstructing

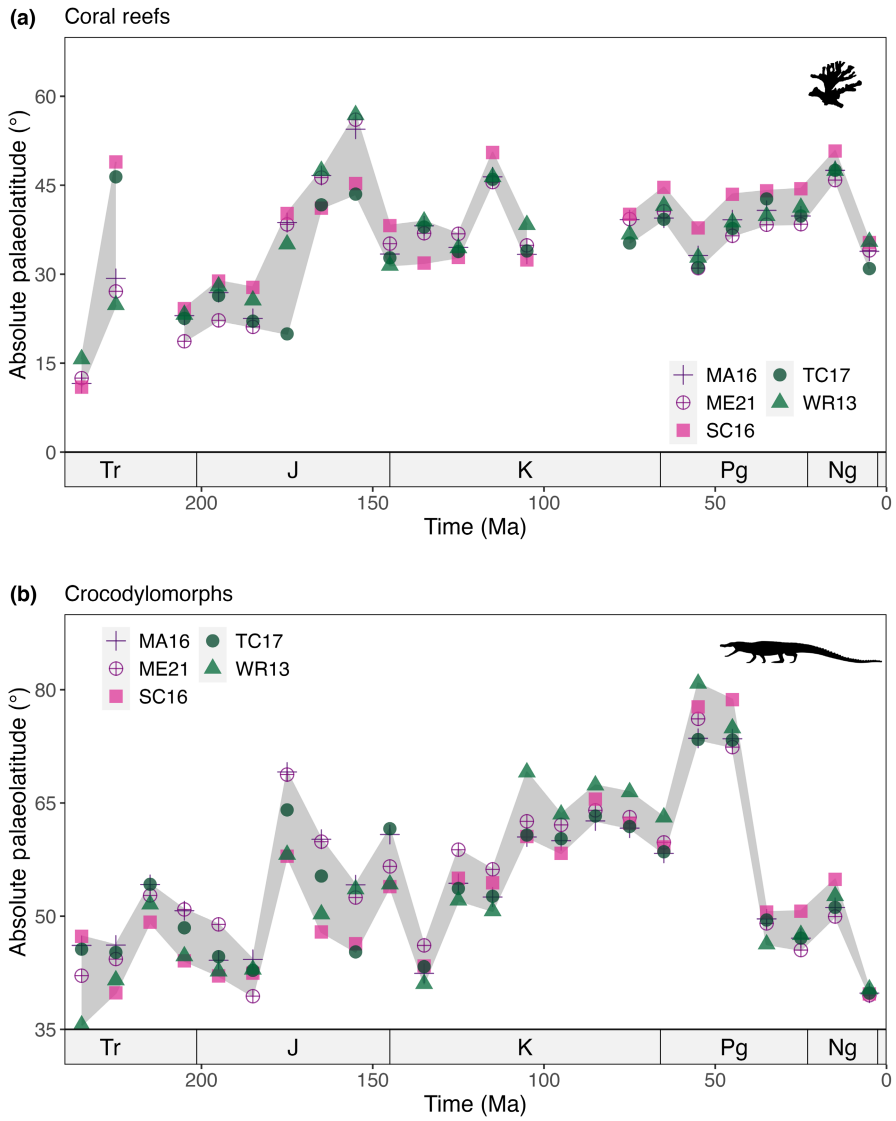

FIGURE 5 Palaeogeographic uncertainty in fossil-based reconstruction of the (sub-)tropics within 10 Myr time steps (0–240 Ma). For each time step, the maximum absolute reconstructed palaeolatitude of coral reefs with a tropical affinity (a) and terrestrial crocodylomorphs (b) is depicted for each global plate model. The uncertainty of the palaeolatitudinal limit of subtropical reconstruction is depicted as the range between the maximum absolute palaeolatitudes (grey ribbon), with an average uncertainty of 7.7° for coral reefs (a) and 6.5° for crocodylomorphs (b). Both time series exhibit a strong positive correlation between age of reconstruction and palaeolatitudinal uncertainty ($R = 0.43–0.55$; $p \leq 0.05$). Global plate model abbreviations are the same as in Figure 1. The geological time scale axis was added to the plot using the R package 'deeptime' ver. 1.0.1 (Gearty, 2023). Organism silhouettes are from PhyloPic (https://www.phylopic.org/; T. Michael Keesey, 2023) and were added using the rphylopic R package (Gearty & Jones, 2023). Silhouettes were contributed by Scott Hartman, 2011 (CC BY-NC-SA 3.0) and Victor Piñon-González, 2023 (CC0 1.0).

deep-time macroecological trends such as geographic range sizes (e.g. Antell et al., 2020), latitudinal biodiversity gradients (e.g. Powell, 2009; Zhang et al., 2022), and organisms' spatial response to global climatic change (e.g. Reddin et al., 2018). However, the issue of palaeogeographic uncertainty also has relevance for fields such as palaeoclimatology, where palaeotemperature proxies are used to reconstruct latitudinal temperature gradients (e.g. Zhang et al., 2019) and evaluate the performance of palaeoclimatic simulations (e.g. Lunt et al., 2021). Therefore, in the wake of additional methodological concerns that have been considered recently—for example, spatial sampling bias in the geological record (e.g. Close et al., 2020; Jones & Eichenseer, 2021; Vilhena & Smith, 2013)—our work raises a new challenge for those working with fossil data in deep time. Following our results, we recommend that studies dealing with deep-time palaeogeographic reconstructions should consider the robustness of their conclusions to GPM choice (e.g. Boddy et al., 2022), particularly for intervals older than ~300 Ma. Moreover, akin to phylogenies, we advocate that reconstructed coordinates should be treated as the model-based estimates they are, rather than empirical data.

4.2 | Spatial clusters of palaeogeographic uncertainty

Our results show that palaeogeographic reconstruction discrepancies are not only uneven in time but also in space. During the Cenozoic and Mesozoic, high palaeogeographic uncertainty is clustered around active plate boundaries and tectonically complex regions such as along the Eurasian–Indian, Eurasian–Arabian and North American–Juan de Fuca plate boundaries (Figure 4; Figure S4). The high uncertainty values found in these areas are a direct result of differential partitioning in GPMs with cell centroids assigned to different geometries, each with their own unique reconstruction history (Figure S1). This finding suggests that additional caution is warranted when reconstructing the palaeogeographic distribution of fossil occurrences originating from areas close to plate boundaries or within tectonically complex regions. Hence, reconstructions of fossil occurrences from cratonic areas—stable interior portions of continents—ought to be more consistent between GPMs than reconstructions of fossil occurrences from continental margins or the edges of tectonic

blocks. However, our results also suggest that there is an overarching trend of increasing uncertainty among GPMs throughout the Palaeozoic, even in cratonic areas. Rather than differences in the delineation of static polygons, this reflects differences in the modelled rotation histories as prescribed by the rotation files.

4.3 | Pre-Jurassic palaeolongitudinal uncertainty

The direct reconstruction of palaeolongitude is challenging for most of the Earth's history. While palaeomagnetic data can be used to constrain the absolute palaeolatitudinal position of plates and continents, they cannot directly constrain palaeolongitude (Vérard, 2019). Hotspot tracks, which record the motion of a tectonic plate over a mantle plume, enable the determination of palaeolongitude (with respect to the underlying mantle), but owing to the incessant recycling of oceanic crust, well-resolved hotspot tracks are limited to the last ~130 Ma (Seton et al., 2023). Marine magnetic anomalies enable the determination of relative palaeolongitude back to the time of Pangaea breakup (~200 Ma), but they cannot constrain absolute palaeolongitude. Other attempts to constrain palaeolongitude in deeper time remain controversial (Mitchell et al., 2012; Torsvik, Steinberger, et al., 2008). This has broad implications for palaeobiological studies such as those reconstructing organisms' geographic range sizes in deep time (e.g. Kiessling & Aberhan, 2007). However, this will only be an issue in cases where occurrences span a relatively wide number of terranes. Nevertheless, one should also bear in mind that the palaeolatitudinal distribution of the continents can also vary significantly between GPMs particularly in the Palaeozoic (Figure S5), likely resulting from increasing sparsity of palaeomagnetic data over that period, as shown by Torsvik et al. (2012).

4.4 | Reconstructing palaeoclimatic conditions

Fossil occurrences of climatically sensitive organisms are routinely used to estimate the distribution of past climatic conditions (e.g. Burgener et al., 2023; Frakes et al., 1992; Scotese et al., 2021). Here, using five different GPMs, we estimated the palaeolatitudinal extent of (sub-)tropical climatic conditions for the last 240 Myr using fossil terrestrial crocodylomorphs and warm-water coral reefs (Figure 5). Our findings support previous work in demonstrating that GPM choice can strongly influence reconstructions of palaeoclimatic conditions when based on geological data (e.g. Cao et al., 2019). Moreover, our results suggest that previous conclusions based on the use of one GPM might be worth revisiting (e.g. Kiessling, 2001; Markwick, 1998). Nevertheless, while large differences (~24.1° latitude) can be observed between GPMs in extreme cases, the direction of change (equatorward vs. poleward) is largely consistent between GPMs suggesting broad-scale relative patterns are constrained. Consequently, across temporal scales, the use of a single GPM can be useful for informing relative changes within a time series, but the magnitude of change relative to the present-day should be carefully considered.

4.5 | Study limitations

We quantified Phanerozoic (540–0 Ma) palaeogeographic uncertainty between five GPMs using a global hexagonal grid (~100 km spacings). While the use of additional models such as the commonly applied Getech plate model would be desirable to further quantify palaeogeographic uncertainty (e.g. Chiarenza et al., 2019; Saupe et al., 2019), not all GPMs are open access and broadly available to the community. Despite this, the use of additional models is unlikely to change the general trends observed in this study which are primarily driven by limited data availability (e.g. palaeomagnetic data and constraints on palaeolongitude) and geological interpretation (e.g. tectonic boundaries). Furthermore, the spatial resolution of our study (~100 km spacings) may influence our results in the identification of areas of high palaeogeographic uncertainty. For example, along geological boundaries, a finer scale grid might further constrain the areal extent of these areas. Nevertheless, our results provide a first-order advisory note for those working with spatial data and advocates for the quantification of palaeogeographic uncertainty for individual data sets.

4.6 | Perspectives

Our study provides a primer on GPMs for palaeobiologists and reveals the empirical palaeogeographic uncertainty between the most commonly applied models. A recent review provides an extensive history of the development of plate tectonic modelling, as well as the additional diversity of models available and the working groups in the field (Vérard, 2019). More recently, a technical review was published with the aim of providing a set of principles on how to use—but not abuse—GPMs and their results (Seton et al., 2023). These two reviews provide an excellent summary and guidelines for those getting started with applying GPMs. There is no 'one-size-fits-all' solution when it comes to reconstructing the palaeogeographic distribution of fossil occurrences with GPMs. However, regardless of which GPM is used, we strongly advise that only models provided in a palaeomagnetic reference frame be used for reconstructing palaeocoordinates as they report true palaeolatitudes (typically requires pure palaeomagnetic constraints). Furthermore, we advise consideration of palaeogeographic uncertainty between models along with evaluation of the potential impact of model choice on conclusions. To help facilitate this process, we have made available the 'palaeorotate()' function in the R package palaeoverse (Jones et al., 2023). This function enables users to conveniently generate palaeocoordinates and measures of palaeogeographic uncertainty for their data by making calls to the GPlates Web Service (https://gwsdoc.gplates.org).

5 | CONCLUSION

In conclusion, our study demonstrates that differences in palaeogeographic reconstruction increase with age. Consequently, an increasing level of caution is warranted when reconstructing fossil assemblages from older intervals, particularly for intervals older than ~300 Ma. On average, palaeogeographic reconstructions are in good agreement for the last 100 million years (<5°; <1000 km). However, in older intervals, such as the Cambrian, agreement between palaeogeographic reconstructions is still poor. Despite this, consideration is also required—even for younger intervals—for fossil occurrences originating from tectonically complex regions where the definition of tectonic boundaries lack consensus between global plate models. Our study also demonstrates the impact global plate model choice can have on broader conclusions such as reconstructions of palaeoclimatic conditions based on fossil occurrence data. Therefore, we endorse that studies (e.g. palaeobiology and palaeoclimatology) dependent on deep-time palaeogeographic reconstructions should only use models based on a palaeomagnetic reference frame to reconstruct fossil palaeocoordinates, test the sensitivity of their conclusions to global plate model choice, and quantify the palaeogeographic uncertainty associated with their data.

AUTHOR CONTRIBUTIONS

Lewis A. Jones and Sara Varela conceived the project. All authors contributed to developing the project. Lucas Buffan, Lewis A. Jones and Mathew Domeier wrote the code, conducted the analyses and produced the figures. All authors contributed to writing the manuscript.

ACKNOWLEDGEMENTS

We are grateful for the efforts of all those who have contributed to collecting the fossil data used in this study and entering them into the Paleobiology Database and the PaleoReefs Database. L.B. was funded by the École Normale Supérieure de Lyon, France. L.A.J. and S.V. were funded by the European Research Council under the European Union's Horizon 2020 research and innovation program (grant agreement 947921) as part of the MAPAS project. L.A.J. was also supported by a Juan de la Cierva-formación 2021 fellowship (FJC2021-046695-I) funded by MCIN/AEI/10.13039/501100011033 and the European Union NextGenerationEU/PRTR. M.D. was supported by the Research Council of Norway's Centres of Excellence funding scheme through projects 223272 (CEED) and 332523 (PHAB). S.Z. was supported by Australian Research Council grant DE210100084. (py)GPlates development is funded by the AuScope National Collaborative Research Infrastructure System (NCRIS) Program. This is Palaeobiology Database publication no 461. We thank the Universidade de Vigo and CISUG for funding the article processing charges of this manuscript [Correction added on 26 October 2023, after first online publication: Acknowledgements section has been updated.]

CONFLICT OF INTEREST STATEMENT

The authors have no conflict of interest.

PEER REVIEW

The peer review history for this article is available at https://www.webofscience.com/api/gateway/wos/peer-review/10.1111/2041-210X.14204.

DATA AVAILABILITY STATEMENT

The data generated in this study have been included within the paper, its supplementary material, dedicated GitHub repository (https://github.com/LewisAJones/rotation_sensitivity) and associated Zenodo repository (https://doi.org/10.5281/zenodo.8246558) (Buffan et al., 2023).

CODE AVAILABILITY

Reconstruction grids and palaeocoordinates for fossil occurrence data were generated via pygplates run in python version 3.9.7. Data analyses were conducted in R version 4.2.2. The workflow is available both as R scripts and python-based Jupyter notebooks on GitHub (https://github.com/LewisAJones/rotation_sensitivity) and the associated Zenodo repository (https://doi.org/10.5281/zenodo.8246558) (Buffan et al., 2023).

ORCID

Lucas Buffan https://orcid.org/0000-0002-2353-1432
Lewis A. Jones https://orcid.org/0000-0003-3902-8986
Mathew Domeier https://orcid.org/0000-0002-7647-6852
Sabin Zahirovic https://orcid.org/0000-0002-6751-4976
Sara Varela https://orcid.org/0000-0002-5756-5737

REFERENCES

Allen, B. J., Wignall, P. B., Hill, D. J., Saupe, E. E., & Dunhill, A. M. (2020). The latitudinal diversity gradient of tetrapods across the Permo-Triassic mass extinction and recovery interval. *Proceedings of the Royal Society B: Biological Sciences*, *287*, 11–25. https://doi.org/10.1098/rspb.2020.1125

Alroy, J. (2014). Accurate and precise estimates of origination and extinction rates. *Paleobiology*, *40*, 374–397. https://doi.org/10.1666/13036

Antell, G. S., Kiessling, W., Aberhan, M., & Saupe, E. E. (2020). Marine biodiversity and geographic distributions are independent on large scales. *Current Biology*, *30*, 115–121.e5. https://doi.org/10.1016/j.cub.2019.10.065

Boddy, C. E., Mitchell, E. G., Merdith, A., & Liu, A. G. (2022). Palaeolatitudinal distribution of the Ediacaran macrobiota. *Journal of the Geological Society*, *179*, jgs2021-030. https://doi.org/10.1144/jgs2021-030

Boyden, J. A., Müller, R. D., Gurnis, M., Torsvik, T. H., Clark, J. A., Turner, M., Ivey-Law, H., Watson, R. J., & Cannon, J. S. (2011). Next-generation plate-tectonic reconstructions using GPlates. In *Geoinformatics: Cyberinfrastructure for the solid earth sciences* (pp. 95–113). Cambridge University Press.

Brocklehurst, N., Day, M. O., Rubidge, B. S., & Fröbisch, J. (2017). Olson's extinction and the latitudinal biodiversity gradient of tetrapods in the Permian. *Proceedings of the Royal Society B: Biological Sciences*, *284*, 1–8.

Buffan, L., Jones, L. A., Domeier, M., Scotese, C. R., Zahirovic, S., & Varela, S. (2023). rotation_sensitivity: v1.0.0. *Zenodo*. https://doi.org/10.5281/zenodo.8246558

Burgener, L., Hyland, E., Reich, B. J., & Scotese, C. (2023). Cretaceous climates: Mapping paleo-Köppen climatic zones using a Bayesian statistical analysis of lithologic, paleontologic, and geochemical proxies. *Palaeogeography, Palaeoclimatology, Palaeoecology*, *613*, 111373. https://doi.org/10.1016/j.palaeo.2022.111373

Cao, W., Williams, S., Flament, N., Zahirovic, S., Scotese, C., & Müller, R. D. (2019). Palaeolatitudinal distribution of lithologic indicators of climate in a palaeogeographic framework. *Geological Magazine*, *156*, 331–354. https://doi.org/10.1017/S0016756818000110

Chiarenza, A. A., Mannion, P. D., Lunt, D. J., Farnsworth, A., Jones, L. A., Kelland, S.-J., & Allison, P. A. (2019). Ecological niche modelling does not support climatically-driven dinosaur diversity decline before the cretaceous/paleogene mass extinction. *Nature Communications*, *10*, 1–14. https://doi.org/10.1038/s41467-019-08997-2

Close, R. A., Benson, R. B. J., Saupe, E. E., Clapham, M. E., & Butler, R. J. (2020). The spatial structure of Phanerozoic marine animal diversity. *Science*, *368*, 420–424. https://doi.org/10.1126/science.aay8309

Domeier, M. (2016). A plate tectonic scenario for the Iapetus and Rheic oceans. *Gondwana Research*, *36*, 275–295. https://doi.org/10.1016/j.gr.2015.08.003

Domeier, M. (2018). Early Paleozoic tectonics of Asia: Towards a full-plate model. *Geoscience Frontiers*, *9*, 789–862. https://doi.org/10.1016/j.gsf.2017.11.012

Domeier, M., & Torsvik, T. H. (2014). Plate tectonics in the late Paleozoic. *Geoscience Frontiers*, *5*, 303–350. https://doi.org/10.1016/j.gsf.2014.01.002

Domeier, M., & Torsvik, T. H. (2019). Full-plate modelling in pre-Jurassic time. *Geological Magazine*, *156*, 261–280.

Dunne, E. M., Farnsworth, A., Greene, S. E., Lunt, D. J., & Butler, R. J. (2020). Climatic drivers of latitudinal variation in late Triassic tetrapod diversity. *Palaeontology*, *64*, 101–117. https://doi.org/10.1111/pala.12514

Frakes, L. A., Francis, J. E., & Syktus, J. I. (1992). *Climate modes of the Phanerozoic*. Cambridge University Press. https://doi.org/10.1017/CBO9780511628948

Gearty, W. (2023). deeptime: Plotting Tools for Anyone Working in Deep Time. R package version 1.0.1. https://CRAN.R-project.org/package=deeptime

Gearty, W., & Jones, L. A. (2023). rphylopic: An R package for fetching, transforming, and visualising PhyloPic silhouettes. *bioRxiv: The Preprint Server for Biology* https://doi.org/10.1101/2023.06.22.546191

Golonka, J. (2007). Late Triassic and early Jurassic palaeogeography of the world. *Palaeogeography, Palaeoclimatology, Palaeoecology*, *244*, 297–307.

Golonka, J. R., Ross, M. I., & Scotese, C. R. (1994). Phanerozoic paleogeographic and paleoclimatic modeling maps. *Pangea: Global Environments and Resources*, *17*, 1–47.

Gurnis, M., Yang, T., Cannon, J., Turner, M., Williams, S., Flament, N., & Müller, R. D. (2018). Global tectonic reconstructions with continuously deforming and evolving rigid plates. *Computers & Geosciences*, *116*, 32–41. https://doi.org/10.1016/j.cageo.2018.04.007

Hijmans, R. J., Karney (GeographicLib), C., Williams, E., & Vennes, C. (2021). geosphere: Spherical Trigonometry. https://CRAN.R-project.org/package=geosphere

Jones, L. A., & Eichenseer, K. (2021). Uneven spatial sampling distorts reconstructions of Phanerozoic seawater temperature. *Geology*, *50*, 238–242. https://doi.org/10.1130/G49132.1

Jones, L. A., Gearty, W., Allen, B. J., Eichenseer, K., Dean, C. D., Galván, S., Kouvari, M., Godoy, P. L., Nicholl, C. S. C., Buffan, L., Dillon, E. M., Flannery-Sutherland, J. T., & Chiarenza, A. A. (2023). palaeoverse: A community-driven R package to support palaeobiological analysis. *Methods in Ecology and Evolution*, 1–11. https://doi.org/10.1111/2041-210X.14099

Jones, L. A., Mannion, P. D., Farnsworth, A., Bragg, F., & Lunt, D. J. (2022). Climatic and tectonic drivers shaped the tropical distribution of coral reefs. *Nature Communications*, *13*, 3120. https://doi.org/10.1038/s41467-022-30793-8

Kiessling, W. (2001). Paleoclimatic significance of Phanerozoic reefs. *Geology*, *29*, 751–754. https://doi.org/10.1130/0091-7613(2001)029<0751:PSOPR>2.0.CO;2

Kiessling, W., & Aberhan, M. (2007). Geographical distribution and extinction risk: Lessons from Triassic–Jurassic marine benthic organisms. *Journal of Biogeography*, *34*, 1473–1489. https://doi.org/10.1111/j.1365-2699.2007.01709.x

Kiessling, W., & Krause, M. C. (2022). PARED—An online database of Phanerozoic reefs. https://www.paleo-reefs.pal.uni-erlangen.de

Lunt, D. J., Bragg, F., Chan, W. L., Hutchinson, D. K., Ladant, J. B., Morozova, P., Niezgodzki, I., Steinig, S., Zhang, Z., Zhu, J., Abe-Ouchi, A., Anagnostou, E., de Boer, A. M., Coxall, H. K., Donnadieu, Y., Foster, G., Inglis, G. N., Knorr, G., Langebroek, P. M., … Otto-Bliesner, B. L. (2021). DeepMIP: Model intercomparison of early Eocene climatic optimum (EECO) large-scale climate features and comparison with proxy data. *Climate of the Past*, *17*, 203–227. https://doi.org/10.5194/cp-17-203-2021

Lunt, D. J., Farnsworth, A., Loptson, C., Foster, G. L., Markwick, P., O'Brien, C. L., Pancost, R. D., Robinson, S. A., & Wrobel, N. (2016). Palaeogeographic controls on climate and proxy interpretation. *Climate of the Past*, *12*, 1181–1198. https://doi.org/10.5194/cp-12-1181-2016

Mannion, P. D., Benson, R. B. J., Carrano, M. T., Tennant, J. P., Judd, J., & Butler, R. J. (2015). Climate constrains the evolutionary history and biodiversity of crocodylians. *Nature Communications*, *6*, 8438. https://doi.org/10.1038/ncomms9438

Mannion, P. D., Upchurch, P., Benson, R. B. J., & Goswami, A. (2014). The latitudinal biodiversity gradient through deep time. *Trends in Ecology & Evolution*, *29*, 42–50. https://doi.org/10.1016/j.tree.2013.09.012

Markwick, P. J. (1998). Crocodilian diversity in space and time: The role of climate in paleoecology and its implication for understanding K/T extinctions. *Paleobiology*, *24*, 470–497. https://doi.org/10.1017/S009483730002011X

Markwick, P. J. (2007). The palaeogeographic and palaeoclimatic significance of climate proxies for data-model comparisons. In M. Williams, A. M. Haywood, F. J. Gregory, & D. N. Schmidt (Eds.), *Deep-time perspectives on climate change: Marrying the signal from computer models and biological proxies*, *the Geological Society of London on behalf of the micropalaeontological society* (pp. 251–312). Geological Society of London. https://doi.org/10.1144/TMS002.13

Markwick, P. J. (2019). Palaeogeography in exploration. *Geological Magazine*, *156*, 366–407.

Matthews, K. J., Maloney, K. T., Zahirovic, S., Williams, S. E., Seton, M., & Müller, R. D. (2016). Global plate boundary evolution and kinematics since the late Paleozoic. *Global and Planetary Change*, *146*, 226–250. https://doi.org/10.1016/j.gloplacha.2016.10.002

McKenzie, D. P., & Parker, R. L. (1967). The North Pacific: An example of tectonics on a sphere. *Nature*, *216*, 1276–1280.

Merdith, A. S., Collins, A. S., Williams, S. E., Pisarevsky, S., Foden, J. D., Archibald, D. B., Blades, M. L., Alessio, B. L., Armistead, S., Plavsa, D., Clark, C., & Müller, R. D. (2017). A full-plate global reconstruction of the Neoproterozoic. *Gondwana Research*, *50*, 84–134. https://doi.org/10.1016/j.gr.2017.04.001

Merdith, A. S., Williams, S. E., Collins, A. S., Tetley, M. G., Mulder, J. A., Blades, M. L., Young, A., Armistead, S. E., Cannon, J., Zahirovic, S., & Müller, R. D. (2021). Extending full-plate tectonic models into deep time: Linking the Neoproterozoic and the Phanerozoic. *Earth-Science Reviews*, *214*, 103477. https://doi.org/10.1016/j.earscirev.2020.103477

Meseguer, A. S., & Condamine, F. L. (2020). Ancient tropical extinctions at high latitudes contributed to the latitudinal diversity gradient. *Evolution*, *74*, 1–22. https://doi.org/10.1111/evo.13967

Mitchell, R. N., Kilian, T. M., & Evans, D. A. D. (2012). Supercontinent cycles and the calculation of absolute palaeolongitude in deep

time. *Nature*, *482*, 208–211. https://doi.org/10.1038/nature10800

Morgan, W. J. (1968). Rises, trenches, great faults, and crustal blocks. *Journal of Geophysical Research*, *73*, 1959–1982.

Müller, R. D., Cannon, J., Qin, X., Watson, R. J., Gurnis, M., Williams, S., Pfaffelmoser, T., Seton, M., Russell, S. H. J., & Zahirovic, S. (2018). GPlates: Building a virtual earth through deep time. *Geochemistry, Geophysics, Geosystems*, *19*, 2243–2261. https://doi.org/10.1029/2018GC007584

Müller, R. D., Royer, J.-Y., & Lawver, L. A. (1993). Revised plate motions relative to the hotspots from combined Atlantic and Indian Ocean hotspot tracks. *Geology*, *21*, 275–278. https://doi.org/10.1130/0091-7613(1993)021<0275:RPMRTT>2.3.CO;2

Müller, R. D., Seton, M., Zahirovic, S., Williams, S. E., Matthews, K. J., Wright, N. M., Shephard, G. E., Maloney, K. T., Barnett-Moore, N., Hosseinpour, M., Bower, D. J., & Cannon, J. (2016). Ocean basin evolution and global-scale plate reorganization events since Pangea breakup. *Annual Review of Earth and Planetary Sciences*, *44*, 107–138. https://doi.org/10.1146/annurev-earth-060115-012211

Müller, R. D., Zahirovic, S., Williams, S. E., Cannon, J., Seton, M., Bower, D. J., Tetley, M. G., Heine, C., le Breton, E., Liu, S., Russell, S. H. J., Yang, T., Leonard, J., & Gurnis, M. (2019). A global plate model including lithospheric deformation along major rifts and Orogens since the Triassic. *Tectonics*, *38*, 1884–1907. https://doi.org/10.1029/2018TC005462

Powell, M. G. (2009). The latitudinal diversity gradient of brachiopods over the past 530 million years. *The Journal of Geology*, *117*, 585–594. https://doi.org/10.1086/605777

Powell, M. G., Moore, B. R., & Smith, T. J. (2015). Origination, extinction, invasion, and extirpation components of the brachiopod latitudinal biodiversity gradient through the Phanerozoic eon. *Paleobiology*, *41*, 330–341.

Reddin, C. J., Kocsis, Á. T., & Kiessling, W. (2018). Marine invertebrate migrations trace climate change over 450 million years. *Global Ecology and Biogeography*, *27*, 704–713. https://doi.org/10.1111/geb.12732

Saupe, E. E., Farnsworth, A., Lunt, D. J., Sagoo, N., Pham, K. V., & Field, D. J. (2019). Climatic shifts drove major contractions in avian latitudinal distributions throughout the Cenozoic. *Proceedings of the National Academy of Sciences of the United States of America*, *116*, 12895–12900. https://doi.org/10.1073/pnas.1903866116

Scotese, C. (2004). A continental drift flipbook. *Journal of Geology*, *112*, 729–741. https://doi.org/10.1086/424867

Scotese, C., & Wright, N. M. (2018). PALEOMAP paleodigital elevation models (PaleoDEMs) for the Phanerozoic PALEOMAP Project. https://www.earthbyte.org/paleodem-resource-scotese-and-wright-2018/

Scotese, C. R. (2016). Tutorial: PALEOMAP paleoAtlas for GPlates and the paleoData plotter program: PALEOMAP Project, Technical Report.

Scotese, C. R., & Elling, R. (2017). Plate tectonic evolution during the last 1.3 billion years: The movie. In *Burlington house* (pp. 16–17). The Geological Society of London.

Scotese, C. R., Gahagan, L. M., & Larson, R. L. (1988). Plate tectonic reconstructions of the cretaceous and Cenozoic Ocean basins. *Tectonophysics*, *155*, 27–48. https://doi.org/10.1016/0040-1951(88)90259-4

Scotese, C. R., Song, H., Mills, B. J. W., & van der Meer, D. G. (2021). Phanerozoic paleotemperatures: The earth's changing climate during the last 540 million years. *Earth-Science Reviews*, *215*, 103503. https://doi.org/10.1016/j.earscirev.2021.103503

Seton, M., Müller, R. D., Zahirovic, S., Gaina, C., Torsvik, T., Shephard, G., Talsma, A., Gurnis, M., Turner, M., Maus, S., & Chandler, M. (2012). Global continental and ocean basin reconstructions since 200 Ma. *Earth-Science Reviews*, *113*, 212–270. https://doi.org/10.1016/j.earscirev.2012.03.002

Seton, M., Williams, S. E., Domeier, M., Collins, A. S., & Sigloch, K. (2023). Deconstructing plate tectonic reconstructions. *Nature Reviews Earth & Environment*, *4*, 1–20. https://doi.org/10.1038/s43017-022-00384-8

Song, H., Huang, S., Jia, E., Dai, X., Wignall, P. B., & Dunhill, A. M. (2020). Flat latitudinal diversity gradient caused by the Permian–Triassic mass extinction. *Proceedings of the National Academy of Sciences of the United States of America*, *117*, 1–6. https://doi.org/10.1073/pnas.1918953117

Spano, C. A., Hernández, C. E., & Rivadeneira, M. M. (2016). Evolutionary dispersal drives the latitudinal diversity gradient of stony corals. *Ecography*, *39*, 836–843. https://doi.org/10.1111/ecog.01855

Torsvik, T. H., & Cocks, L. R. M. (2017). Earth history and palaeogeography.

Torsvik, T. H., Müller, R. D., Van der Voo, R., Steinberger, B., & Gaina, C. (2008). Global plate motion frames: Toward a unified model. *Reviews of Geophysics*, *46*, 1–44. https://doi.org/10.1029/2007RG000227

Torsvik, T. H., Steinberger, B., Cocks, L. R. M., & Burke, K. (2008). Longitude: Linking Earth's ancient surface to its deep interior. *Earth and Planetary Science Letters*, *276*, 273–282. https://doi.org/10.1016/j.epsl.2008.09.026

Torsvik, T. H., & Van der Voo, R. (2002). Refining Gondwana and Pangea palaeogeography: Estimates of Phanerozoic non-dipole (octupole) fields. *Geophysical Journal International*, *151*, 771–794. https://doi.org/10.1046/j.1365-246X.2002.01799.x

Torsvik, T. H., van der Voo, R., Preeden, U., Mac Niocaill, C., Steinberger, B., Doubrovine, P. V., van Hinsbergen, D. J. J., Domeier, M., Gaina, C., Tohver, E., Meert, J. G., McCausland, P. J. A., & Cocks, L. R. M. (2012). Phanerozoic polar wander, palaeogeography and dynamics. *Earth-Science Reviews*, *114*, 325–368. https://doi.org/10.1016/j.earscirev.2012.06.007

Uber. (2023). h3-py: Uber's H3 Hexagonal Hierarchical Geospatial Indexing System in Python. https://github.com/uber/h3-py.

Vérard, C. (2019). Plate tectonic modelling: Review and perspectives. *Geological Magazine*, *156*, 208–241. https://doi.org/10.1017/S0016756817001030

Vilhena, D. A., & Smith, A. B. (2013). Spatial bias in the marine fossil record. *PLoS ONE*, *8*(10), 1–7. https://doi.org/10.1371/journal.pone.0074470

Williams, S., Cannon, J., Qin, X., & Müller, D. (2017). PyGPlates—A GPlates Python library for data analysis through space and deep geological time. p. 8556.

Wright, N., Zahirovic, S., Müller, R. D., & Seton, M. (2013). Towards community-driven paleogeographic reconstructions: Integrating open-access paleogeographic and paleobiology data with plate tectonics. *Biogeosciences*, *10*, 1529–1541. https://doi.org/10.5194/bg-10-1529-2013

Young, A., Flament, N., Maloney, K., Williams, S., Matthews, K., Zahirovic, S., & Müller, R. D. (2019). Global kinematics of tectonic plates and subduction zones since the late Paleozoic era. *Geoscience Frontiers*, *10*, 989–1013. https://doi.org/10.1016/j.gsf.2018.05.011

Zhang, L., Hay, W. W., Wang, C., & Gu, X. (2019). The evolution of latitudinal temperature gradients from the latest cretaceous through the present. *Earth-Science Reviews*, *189*, 147–158. https://doi.org/10.1016/j.earscirev.2019.01.025

Zhang, S.-H., Shen, S.-Z., & Erwin, D. H. (2022). Latitudinal diversity gradient dynamics during carboniferous to Triassic icehouse and greenhouse climates. *Geology*, *50*, 1166–1171. https://doi.org/10.1130/G50110.1

SUPPORTING INFORMATION

Additional supporting information can be found online in the Supporting Information section at the end of this article.

Figure S1. Continental terrane polygons for global plate models used in this study.

Figure S2. Evolution of the scotese global plate model (2004–2017).

Figure S3. Geographic distribution of fossil coral reefs (a) and terrestrial crocodylomorphs (b).

Figure S4. Categorised maps of the mean pairwise geodesic distance between reconstructed palaeocoordinates of cell centroids from global plate models.

Figure S5. Reconstructed continental areas of the early and late Cambrian according to different global plate models: WR13 (a, b), SC16 (c, d), TC17 (e, f) and ME21 (g, h).

Figure S6. Palaeolatitudinal reconstruction of fossil coral reefs (a) and terrestrial crocodylomorphs (b) according to the five global plate models used in this study.

How to cite this article: Buffan, L., Jones, L. A., Domeier, M., Scotese, C. R., Zahirovic, S., & Varela, S. (2023). Mind the uncertainty: Global plate model choice impacts deep-time palaeobiological studies. *Methods in Ecology and Evolution*, *14*, 3007–3019. https://doi.org/10.1111/2041-210X.14204